Article

pubs.acs.org/Biomac

Synthesis, Characterization, and Biocompatibility of Biodegradable Hyperbranched Polyglycerols from Acid-Cleavable Ketal Group Functionalized Initiators

Rajesh A. Shenoi,[†] Benjamin F. L. Lai,[†] and Jayachandran N. Kizhakkedathu*[,†,‡]

[†]Centre for Blood Research and Department of Pathology and Laboratory Medicine, University of British Columbia, Vancouver BC, Canada V6T 1Z3

[‡]Department of Chemistry, University of British Columbia, Vancouver BC, Canada V6T 1Z3

Supporting Information

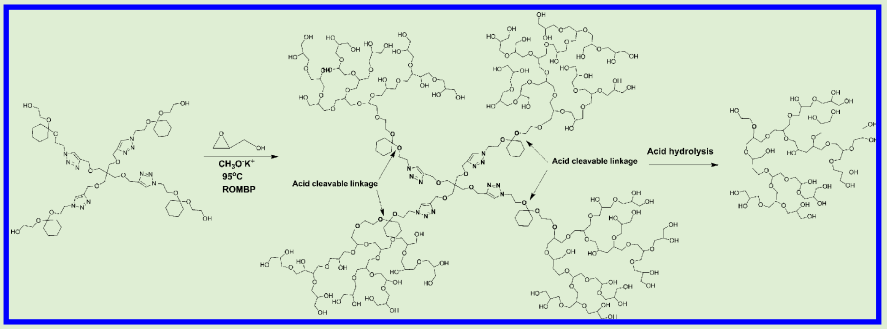

ABSTRACT: Herein we report the synthesis of biodegradable hyperbranched polyglycerols (BHPGs) having acid-cleavable core structure by anionic ring-opening multibranching polymerization (ROMBP) of glycidol using initiators bearing dimethyl and cyclohexyl ketal groups. Five different multifunctional initiators carrying one to four ketal groups and two to four hydroxyl groups per molecule were synthesized. The hydroxyl carrying initiators containing one ketal group per molecule were synthesized from ethylene glycol. An alkyne−azide click reaction was used for synthesizing initiators containing multiple cyclohexyl ketal linkages and hydroxyl groups. The synthesized BHPGs exhibited monomodal molecular weight distributions and polydispersity in the range of 1.2 to 1.6, indicating the controlled nature of the polymerizations. The polymers were relatively stable at physiological pH but degraded at acidic pH values. The polymer degradation was dependent on the type of ketal structure present in the BHPG; polymers with cyclohexyl ketal groups degraded at much slower rates than those with dimethyl ketal groups at a given pH. Good control of polymer degradation was achieved under mild acidic conditions by changing the structure of ketal linkages. A precise control of the molecular weight of the degraded HPG was achieved by controlling the number of ketal groups within the core, as revealed from the gel permeation chromatography (GPC) analyses. The decrease in the polymer molecular weights upon degradation was correlated well with the number of ketal groups in their core structure. Our data support the suggestion that glycidol was polymerized uniformly from all hydroxyl groups of the initiators. BHPGs and their degradation products were highly biocompatible, as measured by blood coagulation, complement activation, platelet activation, and cell viability assays. The controlled degradation profiles of these polymers together with their excellent biocompatibility make them suitable for drug delivery and bioconjugation applications.

1. INTRODUCTION

In the past few years there has been considerable advancement in the use of dendritic and hyperbranched polymers for a variety of biomedical applications including drug delivery, tissue engineering, protein delivery, and gene transfection.[1−6] Among these, hyperbranched polyglycerols (HPGs) have received much attention recently due to their special features.[7−9] HPGs possess dendrimer-like properties and could be synthesized by a single-step process and have a compact globular structure. The most common method employed for the synthesis of HPGs involves the anionic ring-opening multibranching polymerization (ROMBP) of glycidol using a multifunctional initiator, 1,1,1-tris(hydroxymethyl)propane (TMP), which is partially deprotonated using potassium methoxide.[10] Slow addition of monomer to a partially deprotonated multifunctional initiator results in polymers with controlled molecular weights and narrow polydispersity. Polymers of varying molecular weights are accessible through the proper choice of the polymerization conditions such as the use of 1,4-dioxane as an emulsifier for achieving very high molecular weights (300−1000 kDa)[11] or employing macro-initiators for the synthesis of medium molecular weight HPGs

Received: March 23, 2012
Revised: August 20, 2012

   dx.doi.org/10.1021/bm300959h | *Biomacromolecules* XXXX, XXX, XXX−XXX

(6−25 kDa).[12] Haag and coworkers recently reported the synthesis of cross-linked HPG particles of size varying from a few nanometers to several micrometers using miniemulsion and microfluidic template technologies.[13] HPGs are shown to be highly biocompatible, and a large number of hydroxyl groups in the polymers serve as potential sites for the conjugation of drugs and bioactive molecules such as peptides and carbohydrates.[14−22] HPGs with hydrophobic alkyl groups in the core have been designed for applications such as human serum albumin (HSA) substitute[23] and the encapsulation of hydrophobic drugs and several guest molecules.[24−28] Functionalization of HPGs with cationic groups has shown potential for the delivery of nucleic acids as they bind DNA and condense them into smaller particles (<100 nm).[29,30] There have also been reports on the use of HPGs modified with anionic groups as heparin analogues and as anti-inflammatory agents.[31−33] It has been demonstrated that grafting of red blood cells (RBCs) to HPGs results in increased antigen protection on the RBC surfaces.[34−36] The use of aldehyde-functionalized HPGs as soluble peptide capture agents in proteomic analysis has been studied.[37,38] There is also a recent report on the conjugation of choline phosphate to HPG and its use as a universal biomembrane adhesive.[39] All of these studies demonstrate the versatility of HPGs for a variety of applications in bio/nanomedicine.

Another attractive feature that makes HPGs suitable for drug delivery is that their circulation half-lives in vivo can be controlled by varying the molecular weights. For example, HPGs of molecular weight 100 kDa and 500 kDa have circulation half-lives of 32 h and 57 h, respectively.[40] The conjugation of drugs to such high-molecular-weight polymers may result in better bioavailability of the drugs due to the longer circulation times that in turn lead to better therapeutic efficiency. In addition to this, conjugation of proteins or carbohydrates to high-molecular-weight HPGs leads to multivalent interactions with proteins and cells.[21,22] Despite these advantages, in vivo studies have revealed relatively higher levels of accumulation for higher molecular weight HPGs in organs such as liver,[39] 10−14% of injected dose was accumulated in the liver. The organ accumulation decreased with decreasing molecular weight.[39] Also, the glomerular filtration limit for polymers is in the range of 50−65 kDa. This necessitates the need for designing biodegradable versions of HPGs for the development of long circulating drug delivery vehicles. Also, controlling the molecular weight of the degraded fragment will facilitate the clearance of these polymers via kidney without organ accumulation and without affecting their biocompatibility profile. This can be achieved by incorporating defined degradation points within the polymer. One such approach towards synthesizing biodegradable HPG nanogels has been reported by Haag and coworkers using disulfide as the degradable linkage that can be cleaved under the reductive environment within cells.[41] Acid-catalyzed miniemulsion polymerization of triglycidyl ether with disulfide containing cross-linkers was used for the synthesis of these biodegradable HPG nanogels. However, there are no reports on the synthesis of soluble biodegradable HPGs without the use of cross-linkers.

Here we report the synthesis of biodegradable hyperbranched polyglycerols (BHPGs) using novel multifunctional initiators containing different numbers of acid degradable dimethyl and cyclohexyl ketal linkages in their structure. This is the first report of ketal-group-containing HPGs. We selected acid-degradable ketal group as the degradable moiety due to the broad range of applications of pH sensitive polymers as delivery vehicles for antitumor agents, proteins and nucleic acids as well as for the treatment of acute inflammatory diseases. pH-sensitive polymers could be more efficient in tumor targeting due to the acidic environment of most tumor cells. Protein and nucleic acid delivery requires the endosomal degradation of the polymeric carrier and release of the therapeutic molecule to the cytosol.[42−46] The ketal groups can undergo degradation under the mild acid conditions of the cellular compartments such as endosomes.[47] In this article, we report the synthesis of five different ketal-containing initiators. BHPGs were synthesized by the anionic ROMBP of glycidol using these initiators. We have investigated polymerization of glycidol from different initiators and studied their degradation behavior. The control over polymer degradation was achieved using different ketal linkages in the polymer. We have also investigated the cell compatibility and hemocompatibility of the degradable HPGs and their degradation products.

2. EXPERIMENTAL SECTION

2.1. Materials. Ethylene glycol (anhydrous, 99.8%), trimethyl orthoacetate (99%), *p*-toluene sulfonic acid monohydrate (ACS reagent, ≥98.5%), pyridinium *p*-toluenesulfonate (98%), molecular sieves 5 Å, 2-methoxy propene (97%), trimethyl orthoformate (99%), cyclohexanone (99.5%), 2-bromoethanol (95%), glycerol (99.5%), pentaerythritol (98%), diethylene glycol (≥99%), copper sulfate pentahydrate (ACS reagent, ≥98%), sodium ascorbate (≥98%), and potassium methoxide (25% solution in methanol) were all purchased from Sigma-Aldrich, Ontario and were used without further purification. Glycidol (96%) (Sigma-Aldrich) was distilled under reduced pressure before use and stored over molecular sieves at 4 °C. Dichloromethane, diethyl ether, tetrahydrofuran, methanol, hexane and ethyl acetate were procured from Fisher Scientific, Canada. Ethylene glycol monoacetate,[48] 2-azido ethanol,[49] 1-Methoxycyclohexene,[50] bis(2-propynoxyethyl)ether,[51] tris(2-propynoxy)propane[51] and tetrakis(2-propynoxymethyl)methane[51] were synthesized as per the previously reported literature.

2.2. Characterization. High-resolution mass spectra of the compounds were recorded on a Waters/Micromass LCT time-of-flight mass spectrometer. NMR spectra of the initiators were recorded in $CDCl_3$ on a Bruker Avance 300 MHz NMR spectrometer. NMR spectra of the polymers were recorded in D_2O or CD_3OD. Inverse-gated (IG) ^{13}C NMR spectra of the polymers were done in deuterated methanol (CD_3OD) with a relaxation delay of 6 s. Molecular weights of the polymers were determined by gel permeation chromatography (GPC) on a Waters 2695 separation module fitted with a DAWN EOS multiangle laser light scattering (MALLS) detector coupled to an Optilab DSP refractive index detector, both from Wyatt Technology. Molecular weight and polydipsersity of the polymers were measured using GPC-MALLS in 10 mM phosphate-buffered 0.1 M $NaNO_3$ at pH 8.5. The analysis was performed using Waters Ultrahydrogel columns (guard, linear and 120) as the mobile phase. We measured the dn/dc of BHPG-DM-1, and it was found to be 0.12, which is similar to that of HPG. The dn/dc value of the polymers is expected to be similar because the initiator content in the polymer is about 5−12%. The degree of branching of the polymers was calculated according to the previously reported literature.[10] To study the pH-dependent degradation, we prepared polymer solutions in buffer solutions in D_2O having pH 1.1−8.2. pH 1.1 buffer was prepared using potassium chloride and HCl, and pH 4.1 buffer was prepared using potassium hydrogen phthalate and sodium hydroxide. Potassium dihydrogen phosphate and sodium hydroxide were used for the preparation of buffer solutions of pH between 5.5 and 8.2. For the polymer degradation studies using NMR analysis, 12−15 mg of the polymer was dissolved in the respective buffer, and their NMR spectra were recorded at various time intervals. The percentage of degradation was calculated from the ratio of the intensities of the peaks

corresponding to ketal group in the polymer and ketone groups generated during the degradation.

2.3. Synthesis of Functional Initiators. *2.3.1. Synthesis of 2,2′-[Propane-2,2-diylbis(oxy)] Diethanol (DMKI-1).* Ethylene glycol monoacetate was synthesized as per reported procedure.[48] Ethylene glycol (30 mL, 0.537 mol), trimethyl orthoacetate (90 mL, 0.698 mol), and *p*-toluene sulfonic acid (2 g) were dissolved in 600 mL of dichloromethane and stirred at room temperature for 4 h. Water (12.6 mL, 0.698 mol) was added to the reaction mixture and stirred for an additional 1 h. Dichloromethane was removed under reduced pressure, and the product 2-hydroxyethylacetate (**2**) was purified by flash chromatography on silica gel using chloroform/acetone (9:1). Yield: 70%. ^{1}H NMR ($CDCl_3$, 300 MHz, δ): 2.09 (s, 3H), 3.83 (t, 2H), 4.19 (t, 2 H). Compound **2** (22 g, 0.211 mol) was dissolved in 300 mL of THF. Pyridinium *p*-toluenesulfonate (PPTS, 2.2 g, 0.00844 mol) was added and stirred for 15 min, followed by the addition of molecular sieves (5 Å) (100 g) and stirring for an additional 15 min. To this mixture, 2-methoxypropene (8.4 mL, 0.0844 mol) was added, and the reaction mixture was stirred at room temperature for 48 h. THF was removed under reduced pressure to yield propane-2,2-diylbis-(oxyethane-2,1-diyl)diacetate (**3**) as a pale-yellow liquid. Yield: 60%. ^{1}H NMR ($CDCl_3$, 300 MHz, δ): 1.38 (s, 6H) 2.07 (s, 6H), 3.64 (t, 4H), 4.18 (t, 4 H).

Deprotection of acetyl group in compound **3** was carried out by treating with sodium hydroxide in methanol/water at room temperature. After the reaction, brine was added and the product was extracted with dichloromethane. Evaporation of dichloromethane under reduced pressure yielded 2,2′-[propane-2,2- diylbis(oxy)] diethanol (**4**) as yellow viscous oil. Yield: 40%. ^{1}H NMR ($CDCl_3$, 300 MHz, δ): 3.71 (t, 4H), 3.58 (t, 4H), 1.38 (s, 6H). ^{13}C NMR ($CDCl_3$, 75 MHz, δ): 99.42, 61.65, 60.93, 24.17. HRMS: Calculated for $[C_7H_{16}O_4+Na]$: 187.0946; found: 187.0945.

2.3.2. Synthesis of 2,2′-[Cyclohexane-2,2-diylbis(oxy)] Diethanol (CHKI-1). 1-Methoxy cyclohexene was synthesized as per the literature procedure.[50] *p*-Toluene sulfonic acid (0.50 g) was added slowly to a mixture of cyclohexanone (**5,** 20 mL, 0.193 mol) and trimethyl orthoformate (30 mL, 0.274 mol) and stirred at r.t. (22 °C) overnight. It was then connected to a fractional distillation unit with a long vigreux column, and the reaction mixture was distilled at atmospheric pressure. Methanol and methyl formate were removed as first fraction, followed by unreacted trimethyl orthoformate. The fraction that distilled at 125−138 °C was collected as pure 1-methoxy cyclohexene (**6**). To a solution of ethylene glycol monoacetate (5.2 g, 0.05 mol) in THF (75 mL) was added *p*-toluene sulfonic acid (0.50 g, 0.0026 mol) and 5 Å molecular sieves (25 g) and stirred for 15 min. Compound **6** (2.2 g, 0.0196 mol) was added, and the reaction mixture was stirred at r.t. for 48 h. Sodium bicarbonate (0.5 g) was added and stirred for 15 min, and the reaction mixture was filtered through a pad of K_2CO_3 kept over Celite bed. The filtrate was evaporated to obtain the crude product, which was purified by column chromatography on silica gel using 5% ethyl acetate in hexane as the eluent. Yield: 46%. ^{1}H NMR (300 MHz, $CDCl_3$, δ): 4.2 (t, 4H), 3.6 (t, 4H), 2.1 (s, 6H), 1.66 (m, 4H), 1.59 (m, 4H), 1.51(m, 2H). ^{13}C NMR (75 MHz, $CDCl_3$, δ): 170.9, 100.3, 63.8, 57.8, 33.4, 22.7, 21.9.

To a stirred solution of the product obtained in the previous step in methanol, potassium carbonate and water were added and stirred at r.t. for 15 h. Reaction mixture was filtered through Celite bed, washed with methanol, and concentrated. The residue obtained was triturated with excess diethyl ether (3 × 50 mL), and ether was removed under reduced pressure. The product obtained was triturated again with hexane (2 × 10 mL), and the hexane layer was decanted. The viscous product was then dissolved in diethylether, dried over anhydrous sodium sulfate, filtered, and evaporated to afford pure product, **CHKI-1 (8)** as a white solid. Yield: 90%. ^{1}H NMR ($CDCl_3$, 300 MHz, δ): 3.75 (t, 4H), 3.58 (t, 4H), 1.69 (t, 4H), 1.52 (m, 4H), 1.43(m, 2H). ^{13}C NMR ($CDCl_3$, 75 MHz, δ): 99.23, 60.96, 60.20, 32.73, 24.61, 21.99. HRMS: Calculated for $[C_{10}H_{20}O_4+Na]$: 227.1259; found 227.1261.

2.3.3. Synthesis of CHKI-2. 2-Azidoethanol[49]and bis(2-propynoxyethyl)ether[51] were synthesized as per reported procedure. Ethyleneglycol monoacetate (7.2 g, 0.069 mol) and azidoethanol (6 g, 0.069 mol) were dissolved in THF (200 mL). *p*-Toluene sulfonic acid (1.3 g, 0.0069 mol) was added to this solution and stirred for 10 min. 5 Å molecular sieves (100 g) was then added and stirred for another 10 min. Finally, 1-methoxy cyclohexene (6.2 g, 0.0552 mol) was added, and the reaction mixture was stirred at room temperature for 48 h. Sodium bicarbonate (0.5 g) was added to the mixture, stirred for 15 min, and filtered through a pad of K_2CO_3 kept over Celite bed. The filtrate was evaporated to obtain the crude product, which was purified by column chromatography on silica gel using 10% ethyl acetate/hexane as the eluent. Yield: 40%. ^{1}H NMR ($CDCl_3$, 300 MHz, δ) 1.41−1.68 (m, 10H), 2.06 (s, 3H), 3.36 (t, 2H), 3.61 (m, 4 H), 4.21 (t, 2H). The azido acetate compound (0.5 g, 1.85 mmol) and bis(2-propynoxyethyl)ether (0.112 g, 6 mmol) were dissolved in methanol. To this mixture was added an aqueous solution of $CuSO_4{\cdot}5H_2O$ (0.071 g, 3.6 mmol) and sodium ascorbate (89 mg, 3.6 mmol), and the solution was stirred at room temperature for 48 h. Methanol was removed under reduced pressure; the residue was dissolved in dichloromethane and washed three times with brine. The organic layer was dried over anhydrous sodium sulfate, and methanol was removed under reduced pressure to yield a dark-brown residue. The compound was further purified by column chromatography on silica gel using 5% methanol/dichloromethane as the eluent. Deprotection of the acetyl groups of the compound was done using potassium carbonate in methanol/water mixture using a similar procedure as that described for CHKI-1. Yield: 63%. ^{1}H NMR ($CDCl_3$, 300 MHz, δ): 7.73 (2H), 4.69(4H), 4.52(4H), 3.82(4H), 3.68(8H), 3.59 (4H), 3.18(4H), 1.30−1.65 (m, 20H). ^{13}C NMR ($CDCl_3$, 75 MHz, δ): 144.34, 123.81, 100.07, 70.13, 69.23, 64.14, 61.26, 60.80, 58.07, 50.21, 33.10, 24.98, 22.42. HRMS: Calculated for $[C_{30}H_{52}N_6O_9+Na]$: 663.3693; found 663.3683.

2.3.4. Synthesis of CHKI-3. **CHKI-3** was synthesized by a similar procedure as that for **CHKI-2** using tris(2-propynoxy)propane[51] and azidoethanol[49] (Scheme 2). Tris(2-propynoxy)propane was synthesized as per reported procedure.[51] ^{1}H NMR ($CDCl_3$, 300 MHz, δ): 7.80 (1H), 7.75(2H), 4.78(2H), 4.64(4H), 4.54(6H), 3.84(6H), 3.61(11H), 3.21(6H), 1.30−1.65(30H). ^{13}C NMR ($CDCl_3$, 75 MHz, δ): 144.7, 144.27, 123.88, 100.14, 69.94, 64.41, 63.86, 61.32, 60.86, 58.11, 53.31, 50.25, 33.15, 25.03, 22.49. HRMS: Calculated for $[C_{42}H_{71}N_9O_{12}+Na]$: 916.5120; found 916.5115.

2.3.5. Synthesis of CHKI-4. **CHKI-4** was synthesized by a similar procedure as that for **CHKI-2** using tetrakis(2-propynoxymethyl) methane[51] and 2-azido ethanol.[49] ^{1}H NMR ($CDCl_3$, 300 MHz, δ): 7.72(4H), 4.55(16H), 3.84(8H), 3.61(8H), 3.45(8H), 3.21(8H), 1.30−1.65(40H). ^{13}C NMR ($CDCl_3$, 75 MHz, δ): 144.77, 123.85, 100.24, 68.91, 64.66, 61.32, 61.47, 60.96, 58.19, 50.29, 33.25, 25.13, 22.59. HRMS: Calculated for $[C_{57}H_{96}N_{12}O_{16}+Na]$: 1227.6965; found 1227.6971.

2.4. General Procedure for the Synthesis of Biodegradable Hyperbranched Polyglycerols. Polymerization of glycidol was carried out under an argon atmosphere in a three-necked glass reactor equipped with a mechanical stirrer and a syringe pump. The new initiators were dissolved in methanol, and 15% of the hydroxyl groups were deprotonated by stirring with potassium methoxide (25% solution in methanol) for 30 min. Methanol was removed under reduced pressure for 5 h. The temperature was increased to 95 °C, and glycidol was added very slowly using a syringe pump over several hours. After the complete addition of the monomer, the reaction mixture was stirred for an additional 3 h. The polymer was dissolved in methanol and precipitated twice from acetone and dried in vacuum.

2.5. Blood Compatibility Analysis. Blood from healthy consented unmedicated donors was collected into either a 3.8% sodium citrated tube with a blood/anticoagulant ratio of 9:1 or a serum tube at Centre for Blood Research, University of British Columbia. 'The protocol was approved by University clinical ethical committee. Platelet-rich plasma (PRP) was prepared by centrifuging citrated whole blood samples at 150*g* for 20 min in an Allegra X-22R centrifuge (Beckman Coulter, Canada). Platelet-poor plasma (PPP) was prepared by centrifuging citrated whole blood samples at 1200*g* for 20 min. Serum was prepared by centrifuging whole blood samples

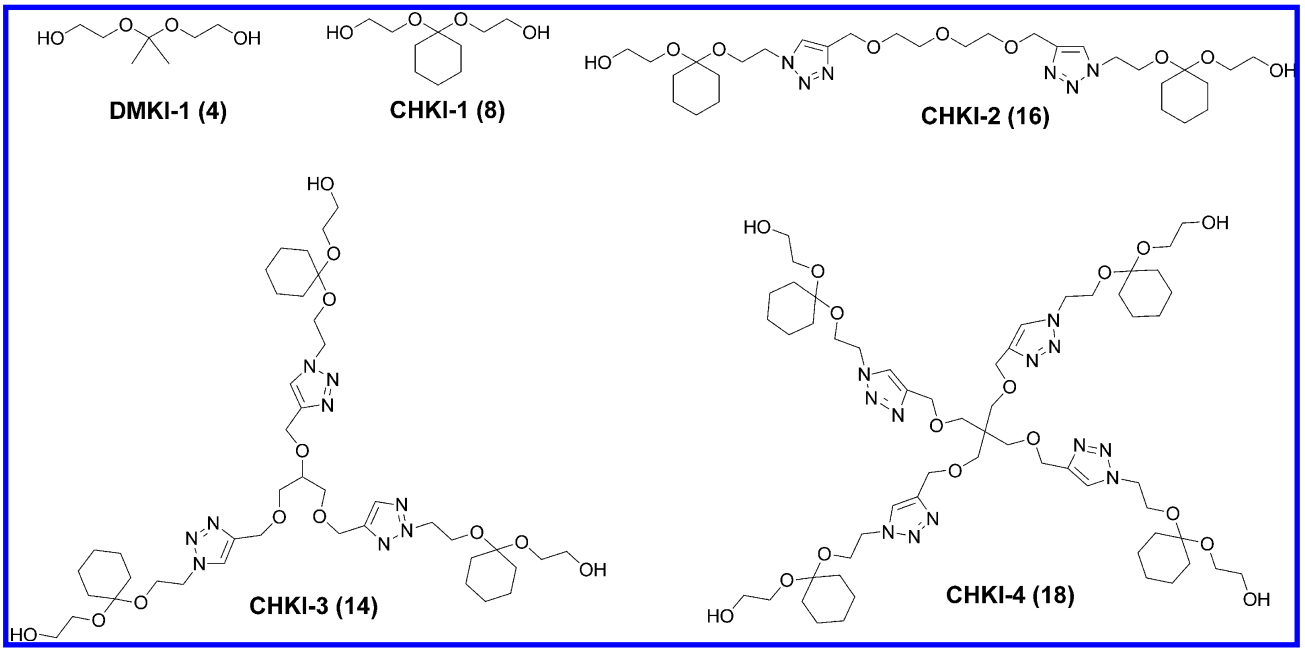

Figure 1. Chemical structures of the hydroxyl functionalized ketal initiators containing one, two, three, and four ketal groups per molecule.

collected in serum tubes at 1200*g* for 30 min. The polymer stock solutions were made in HEPES buffer at a concentration of 10 mg/mL. To make the degraded polymer solution, we prepared BHPG stock solutions in HEPES buffer at 10 mg/mL and kept them at 37 °C for 15 days. It was evident from NMR analysis that the polymers were completely degraded during this time (Supporting Information; Figure S19). The biocompatibility of the degradation products was studied using the completely degraded polymer solutions.

2.5.1. Activated Partial Thromboplastin Time Assay. Sodium citrate anticoagulated PPP was used for activated partial thromboplastin time (APTT) analysis. The effect of BHPGs and their degradation products on the coagulation cascade was examined by mixing PPP with the polymer or degraded polymer solution (9:1 v/v; 1 mg/mL final concentration) at 37 °C. Control experiments were performed with identical volumes of HEPES buffer solution to PPP. The coagulation reagent actin FSL was used for APTT analysis. Each experiment was repeated in triplicates on the STart4 coagulometer (Diagnostica Stago, France) with plasma from three separate donors, and the average ± SD was reported.

2.5.2. Platelet Activation Analysis. The level of platelet activation in PRP was quantified by flow cytometry. PRP (90 μL) was incubated at 37 °C with 10 μL of BHPGs or degraded BHPGs in HEPES buffer to get a final concentration of the polymer 1 mg/mL. After 1 h, aliquots of the incubation mixtures were removed for assessment of the platelet activation state. Postincubation BHPG/platelet mixture (5 μL), diluted in HEPES buffer, was incubated for 20 min in the dark with 5 μL of monoclonal anti-CD62P-PE (Immunotech) and 5 μL of anti-CD42-FITC. The samples were then fixed with 1 mL of formal saline solution (37% formaldehyde in saline). The level of platelet activation was analyzed in a BD FACSCanto II flow cytometer (Becton Dickinson) by gating platelets specific events based on their FITC-CD42 fluorescence and light scattering profile. Activation of platelets was expressed as the percentage of platelet activation marker CD62P-PE fluorescence detected in the 10 000 total events counted. Bovine thrombin (1 U/mL, Sigma) was used as a positive control, and FITC-conjugated and PE-conjugated goat antimouse IgG polyclonal antibodies (Immunotech) were used as the nonspecific binding control. PRP incubated with identical volumes of HEPES as that of the polymer was used a normal control. Duplicate measurements were performed using PRP from three separate donors, and the average ± SD values are reported.

2.5.3. Complement Activation Analysis. The level of complement activation was measured by CH50 sheep erythrocyte lysis assay. Ten microliters each of the BHPG polymers was mixed with 90 μL of fresh human serum for 1 h at 37 °C to get a final concentration of BHPG in serum of 1 mg/mL. Heat-activated human IgG (1 mg/mL) and 5 mM EDTA were positive and negative controls, respectively. HEPES buffer added serum was used as normal control. The postincubation mixture (60 μL) was diluted with 120 μL of GVB^{2+} (CompTech). GVB^{2+} diluted mixture (75 μL) was incubated for 1 h at 37 °C with 75 μL of antibody-sensitized sheep erythrocytes (CompTech). The reaction was stopped by the addition of 300 μL of cold GVB-EDTA to each sample. The samples were centrifuged, and the optical density of supernatant at 540 nm was measured. Distilled water incubated antibody-sensitized sheep erythrocytes was used as 100% lysis control for the calculation. The total complement consumed was measured, and the value is reported as the percent of complement activation.

2.5.4. Cell Viability Analysis. Human umbilical vein endothelial cells (HUVECs) were used to examine the cell viability in presence of BHPGs and their degradation products. The polymers were dissolved in the endothelial cell growth medium (EGM-2 BulletKit, Lonza) media, filtered, and incubated with the cells for 48 h. Starting with an initial polymer concentration of 5 mg/mL, serial dilutions of the polymer solutions with the media were performed to achieve the lower concentrations. Degraded polymer solutions were made by keeping the stock polymer solution in the media for 15 days at 37 °C and then serially diluting the solution with media to obtain different concentrations. HUVECs incubated with the media only were used as the normal control for the study. At the end of the 2-day incubation period, viability was measured by adding 18 μL of the 3-[4,5-dimethylthiazol-2-yl]-5-[3-carboxymethoxyphenyl]-2-[4-sulfophenyl]-2*H*-tetrazolium] (MTS) reagent to each of the wells. The optical density was measured at two wavelengths, 490 and 600 nm. The medium only MTS value was used as the baseline and was expressed as 100% viability. HUVEC viability after exposure to the polymer samples was expressed as the percentage of the cells viable compared with medium-treated cells.

3. RESULTS AND DISCUSSION

3.1. Synthesis of Multifunctional Initiators Containing Ketal Groups. Five different heterofunctional initiators containing dimethyl and cyclohexyl ketal groups in their structure were designed and synthesized (Figure 1). The hydroxyl initiator containing a dimethyl ketal group, **DMKI-1,** was synthesized from ethylene glycol as the starting material

dx.doi.org/10.1021/bm300959h | *Biomacromolecules* XXXX, XXX, XXX–XXX

Scheme 1. Synthetic Route for Multifunctional Initiators with One Ketal Group[a]

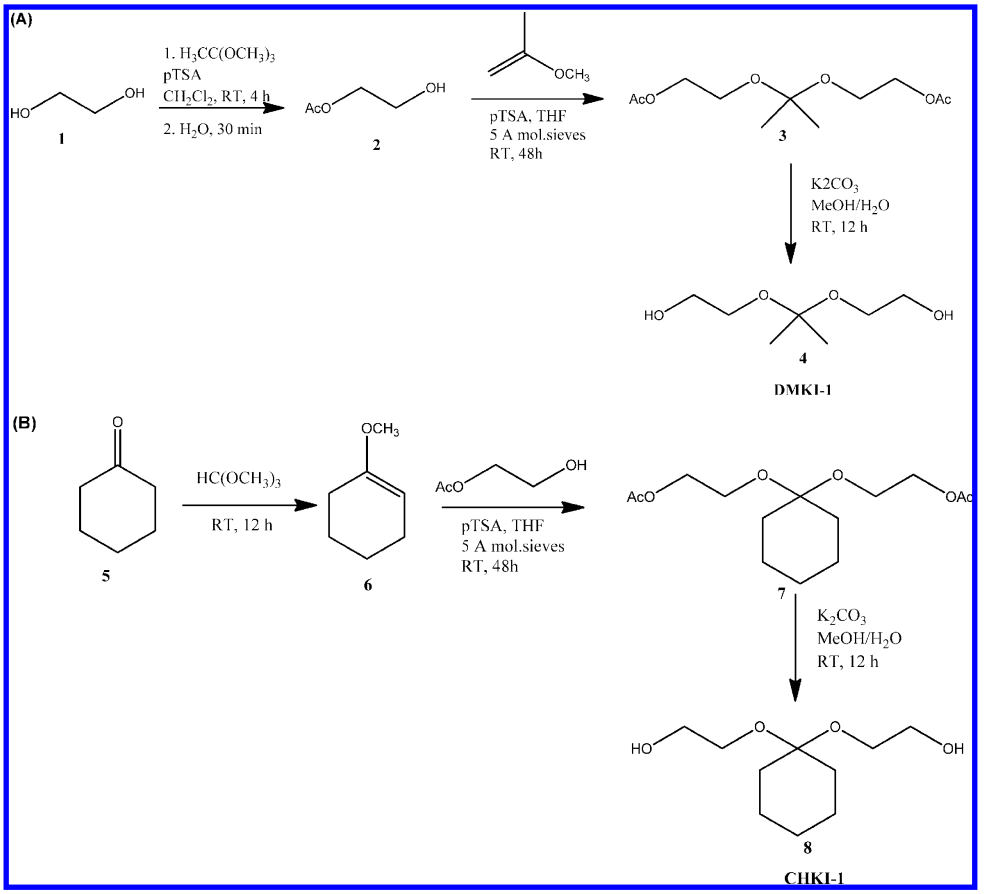

[a](A) 2,2′-[propane-2,2-diylbis(oxy)] diethanol (**DMKI-1**); (B) 2,2′-[cyclohexane-2,2-diylbis(oxy)] diethanol (**CHKI-1**).

(Scheme 1A). Ethylene glycol was first converted to its monoacetate **2** by a reported procedure,[48] which was then reacted with 2-methoxy propene to generate the ketalized diacetate **3.** Deprotection of the acetyl groups with potassium carbonate in methanol/water mixture yielded the compound **4**. The formation of the compound was confirmed by NMR spectroscopy (Supporting Information; Figures S1 and S2) which showed a signal at 1.39 ppm in the ^{1}H NMR spectrum characteristic of the methyl resonance of the dimethyl ketal group (Supporting Information; Figure S1). To synthesize the initiator containing cyclohexyl ketal group, **CHKI-1**, we transformed cyclohexanone into its enol ether **6** by reaction with trimethyl orthoformate in the presence of *p*-toluene sulfonic acid[50] (Scheme 1B). The enol ether was then reacted with ethylene glycol monoacetate to yield the cyclohexyl ketalized diacetate **7**, which upon treatment with potassium carbonate in methanol/water afforded the compound **8**. NMR spectra of the compound **8** are given in the Supporting Information. (See Figures S3 and S4.)

Attempts to synthesize compounds with multiple ketal groups using a similar procedure were not successful. The reaction of trimethylolpropane or pentaerythreitol and ethylene glycol monoacetate with 2-methoxypropene resulted in intramolecular cyclization reactions. So we employed an alkyne−azide click reaction for synthesizing initiators **CHKI-2**, **CHKI-3**, and **CHKI-4** with multiple ketal linkages. A representative synthetic procedure for **CHKI-3** is shown in Scheme 2. In the first step, one equivalent each of ethylene glycol monoacetate and azido ethanol was reacted with 1-methoxy cyclohexene to afford the ketalized azido acetate compound **11**. The trialkyne **12** was synthesized by the reaction of glycerol with propargyl bromide using a reported procedure.[51] The azide **11** and alkyne **12** were reacted in the presence of copper sulfate/sodium ascorbate in methanol/water mixture to yield the compound **13**, which was purified by column chromatography. Deprotection of the acetyl groups of **13** using potassium carbonate in methanol/water afforded the trihydroxy compound **14** with three cyclohexyl ketal linkages. The compound was characterized by ^{1}H NMR that showed signals in the region 7.75 to 7.80 ppm corresponding to the triazole ring proton and those at 1.3 to 1.65 ppm characteristic of the cyclohexyl protons. (See the Supporting Information, Figures S7 and S8.) **CHKI-2** and **CHKI-4** were synthesized using a similar procedure. NMR spectra of the compounds are shown in the Supporting Information. (See Figures S5, S6, S9, and S10.)

3.2. Synthesis of Core-Functionalized BHPGs. All five compounds **DMKI-1**, **CHKI-1**, **CHKI-2**, **CHKI-3**, and **CHKI-4** were investigated as initiators for the anionic ROMBP of glycidol (Scheme 3). The compounds were partially deprotonated (15% of the hydroxyl groups) using potassium methoxide, and polymerizations were carried out at 95 °C with slow monomer addition (Table 1). Polymer yields were in the range of 70−80% with all initiators and were comparable to those reported with trimethylol propane as the initiator. ^{1}H NMR spectra of the polymers showed characteristic signals for the ketal group, which confirmed that the polymer was growing from the ketal-group-containing initiators. The polymer **BHPG-DM-1** obtained from **DMKI-1** initiator showed a signal

dx.doi.org/10.1021/bm300959h | *Biomacromolecules* XXXX, XXX, XXX−XXX

Scheme 2. Synthetic Route for Cyclohexyl Ketal Initiator CHKI-3 Using Azide−Alkyne Click Chemistry

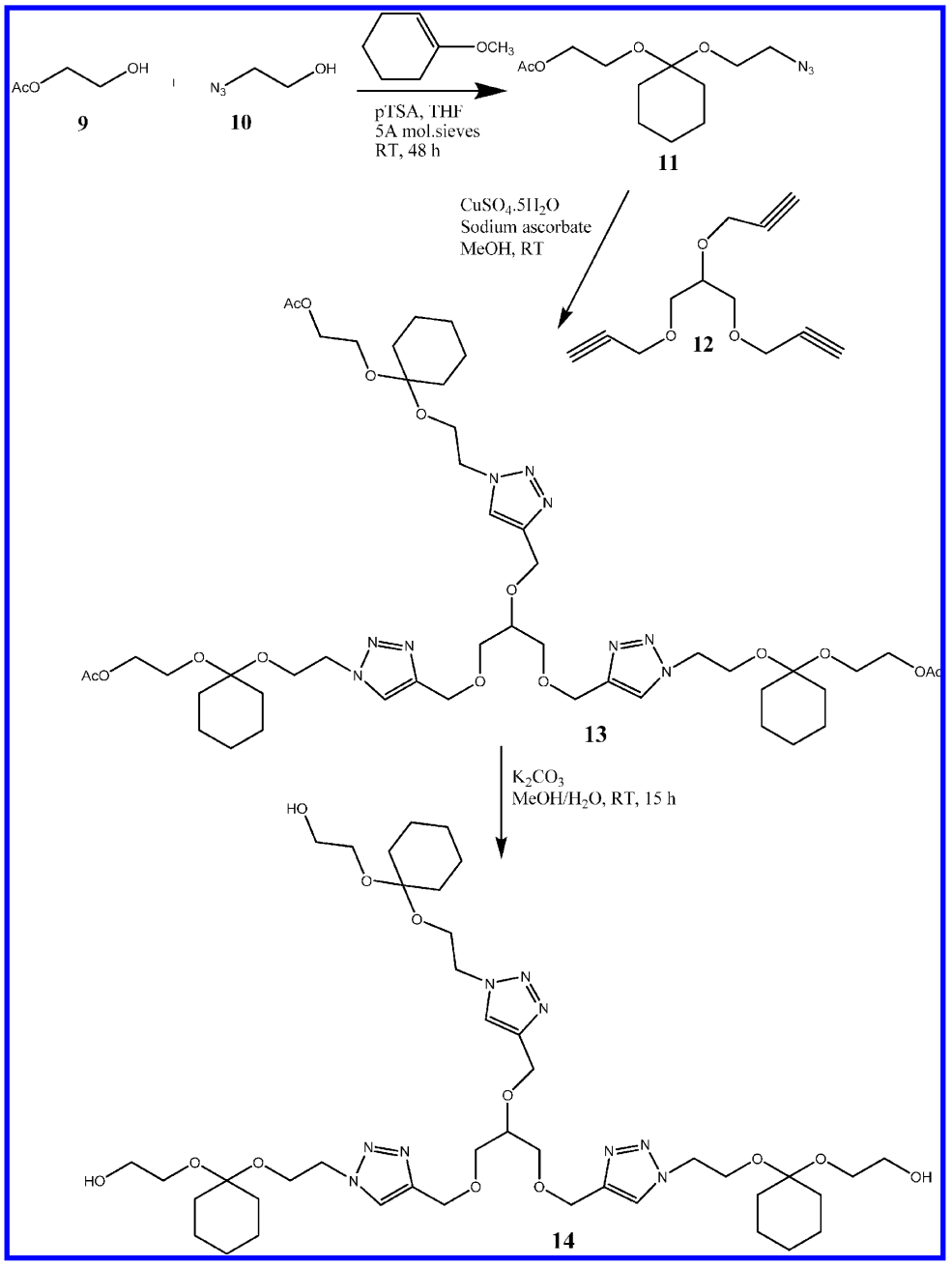

at 1.39 ppm corresponding to the methyl protons of the dimethyl ketal group (Figure 2A and Supporting Information Figure S11). Signals at 1.3 to 1.7 ppm characteristic of the cyclohexyl ketal groups were observed for the polymers **BHPG-CH-1**, **BHPG-CH-2**, **BHPG-CH-3**, and **BHPG-CH-4** obtained from initiators **CHKI-1**, **CHKI-2**, **CHKI-3**, and **CHKI-4**, respectively (Figure 2C and Supporting Information Figures S12−S15). The polymers **BHPG-CH-2**, **BHPG-CH-3**, and **BHPG-CH-4** also showed signals at 8.07, 8.04, and 7.98 ppm, respectively, in the ^{1}H NMR spectra corresponding to the proton of the triazole ring, which further confirms that the growth of the polymer chains was occurring from the initiators.

The branched nature of these polymers was confirmed by inverse gated ^{13}C NMR spectrum (Figure 3); the degree of branching was in the range of 0.54 to 0.58 which was closer to the values reported for HPGs synthesized from TMP initiator.[10] The number of hydroxyl groups on the initiator has no significant effect on the degree of branching. Because ketal groups are known to hydrolyze under acidic conditions, GPC analysis of the polymers was performed in 0.1 N $NaNO_3$ at pH 8.5 to avoid degradation of the polymers during analysis. All polymers exhibited monomodal molecular weight distribution, and the polydispersities were in the range of 1.26 to 1.57 (Table 1). A representative GPC profile for **BHPG-CH-4** is shown in Figure 4, and GPC chromatograms of other polymers are given in the Supporting Information (Figure S16). Results showed that the polymerizations were controlled and glycidol was polymerized uniformly from the initiators.

3.3. Degradation of the Core-Functionalized BHPGs.

After synthesizing BHPGs with well-defined degradation points in their core, we investigated their degradation behavior at different pH values. All of the newly developed BHPGs were

dx.doi.org/10.1021/bm300959h | *Biomacromolecules* XXXX, XXX, XXX−XXX

Scheme 3. Synthetic Route for Biodegradable Hyperbranched Polyglycerol (BHPG-CH-4) Containing Four Ketal Linkages from the Initiator CHKI-4

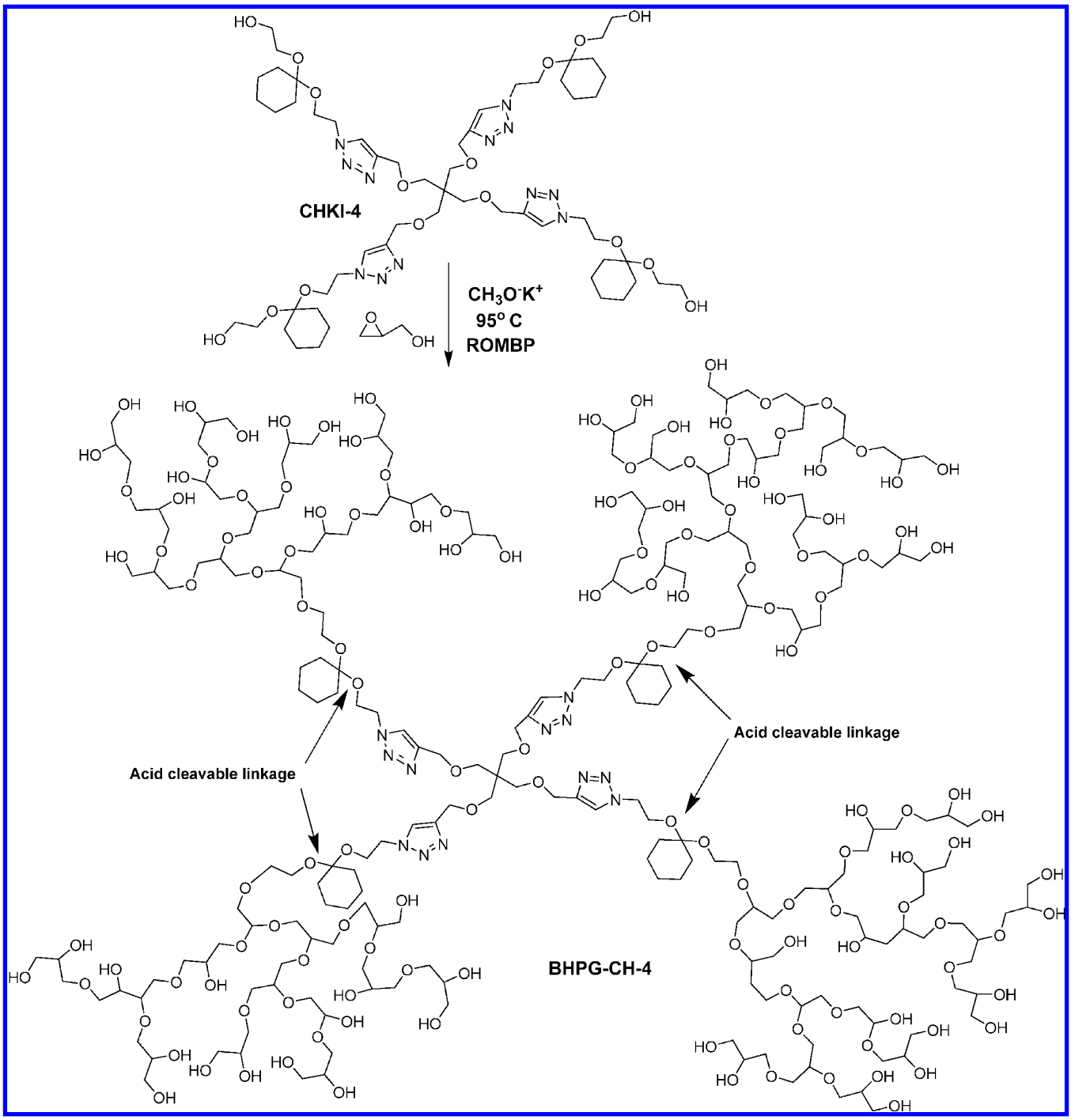

highly soluble in water. The presence of ketal group in the core structure of the polymers makes them susceptible to degradation under acidic conditions, resulting in the formation of low-molecular-weight polymer fragments and small molecular weight ketones. Thus, it is anticipated that polymers **BHPG-DM-1** and **BHPG-DM-2** with dimethylketal groups upon degradation will give two HPG fragments and acetone. The polymers **BHPG-CH-1**, **BHPG-CH-2**, **BHPG-CH-3**, and **BHPG-CH-4** with cyclohexyl ketal groups will degrade to HPG fragments and cyclohexanone. To study the degradation, we dissolved the polymers in deuterated buffers of pH 1.1−8.2, and their NMR spectra were monitored at different time intervals. Degradation of the polymers was evident from the decrease in the intensity of the signal due to ketal group and the appearance of new signals from the ketone released during the degradation. For example, in the case of **BHPG-DM-1**, the signal at 1.39 ppm characteristic of the dimethyl ketal group gradually disappeared with time and a new signal at 2.18 ppm appeared due to the formation of released acetone (Figures 2B and 5). In the case of polymers with cyclohexyl ketal groups, broad signals at 1.3 to 1.7 ppm corresponding to the cyclohexyl groups were shifted to sharper signals at 1.7 and 1.82 ppm, and a new signal was observed at 2.32 ppm due to the cyclohexanone produced during degradation (Figure 2D and

dx.doi.org/10.1021/bm300959h | *Biomacromolecules* XXXX, XXX, XXX−XXX

Table 1. Characteristics of Acid-Cleavable BHPGs Synthesized from Ketal Initiators

polymer	ketal initiator	no. of ketal groups	theoretical molecular weight	M_n (M_w/M_n)		degradation half life at different pH values (h)[a]			
				before degradation	after degradation	5.5	6.0	6.5	7.4
BHPG-DM-1	DMKI-1	1	5000	5200 (1.3)	2800	0.3	1	2.3	32.8
BHPG-DM-2	DMKI-1	1	25000	26000 (1.6)	13 900	n.d.[b]	n.d.	n.d.	n.d.
BHPG-CH-1	CHKI-1	1	10000	9500 (1.26)	4700	2	4.7	13.1	138.6
BHPG-CH-2	CHKI-2	2	5000	4500 (1.24)	2500	1.8	6.6	19.2	168
BHPG-CH-3	CHKI-3	3	10000	7500 (1.57)	2300	4	15.4	27.4	528
BHPG-CH-4	CHKI-4	4	10000	10800 (1.54)	3400	4.3	18.5	30.1	564

[a]Percent of degradation was calculated from ^{1}H NMR spectra by monitoring the disappearance of peaks due to the ketal group in the polymer and appearance of the peaks due to the ketone formed as a result of degradation. The degradation half lives were determined from the plotting $\ln(A/A_0)$ against time, where A_0 is the initial amount of the polymer and A is the concentration of the polymer that is not degraded at a given time t.

[b]n.d.: not determined.

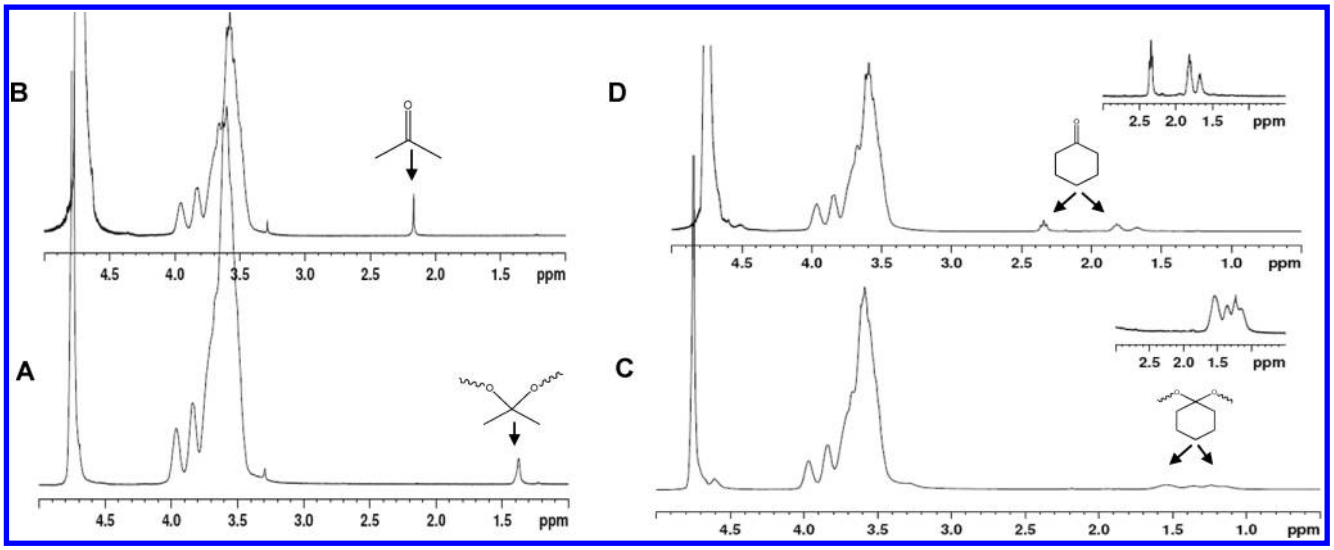

Figure 2. Polymer degradation studied by proton NMR spectroscopy. Shown are ^{1}H NMR spectra of **BHPG-DM-1** and **BHPG-CH-3** before and after degradation. (A) **BHPG-DM-1** before degradation. The signal at 1.39 ppm corresponds to the ketal group. (B) **BHPG-DM**-1 after degradation. The signal at 1.39 ppm due to ketal group disappears completely, and the new signal at 2.18 ppm corresponds to the formation of degradation product acetone. (C) **BHPG-CH-3** before degradation. The signal at 1.3 to 1.6 ppm corresponds to the cyclohexyl protons of the cyclohexyl ketal group. (D) **BHPG-CH-3** after degradation. The signals due to the ketal group completely disappeared, and new sharp peaks appear at 2.32 and 1.65 to 1.85 ppm due to the cyclohexanone formed as a result of degradation.

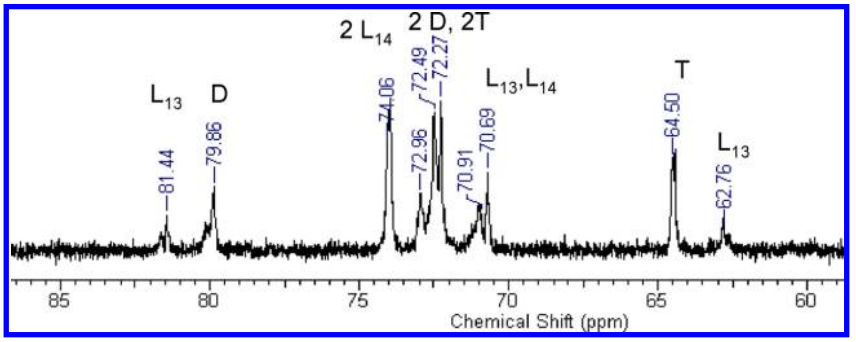

Figure 3. Inverse-gated ^{13}C NMR (CD_3OD, 75 MHz) of **BHPG-CH-3**. The polymer consists of linear (L_{13} and L_{14}), dendritic (D), and terminal (T) structural units. The peak assignments were made according to the literature.[10]

also see the Supporting Information; Figure S17). The time-dependent degradation profiles of the different BHPGs at different pH values are shown in Figure 6. The polymers showed remarkable pH-dependent degradation kinetics; at strongly acidic pH values (1.1 and 4.1), all polymers were completely degraded within the first time point of the NMR experiment (30 min). Controlled degradation profiles were observed in the pH range 5.5−8.2, with slower degradation rates at higher pH values (Figure 6A). The degradation half-lives of the polymers were determined from the plots of $\ln(A/$

dx.doi.org/10.1021/bm300959h | Biomacromolecules XXXX, XXX, XXX−XXX

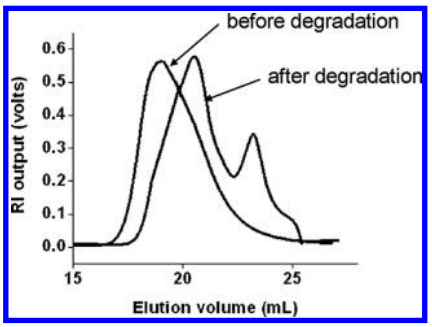

Figure 4. GPC-MALLS chromatograms in 0.1 N $NaNO_3$ at pH 8.5 of **BHPG-CH-4** before and after degradation. The second elution peak for the degraded product could be from the core as the degraded product was not separated before injection. The molecular weight of the degraded product was calculated from the main peak.

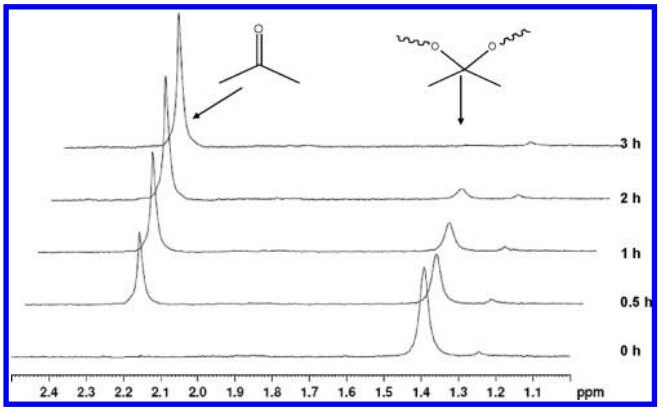

Figure 5. Polymer degradation kinetics by NMR analysis. ^1H NMR spectra (D_2O, 300 MHz) showing the degradation of **BHPG-DM-1** at pH 5.5. The intensity of the signal at 1.39 ppm due to the dimethyl ketal group gradually decreases with time, and a new signal appears at 2.18 ppm due to the formation of acetone as the degradation product.

A_0) against time, where A_0 is the initial amount of the polymer and A is the concentration of the polymer that is not degraded at any given time. The degradation half-lives of the polymers are given in Table 1. The polymer **BHPG-DM-1** with dimethyl ketal group showed degradation half-lives of 0.3, 1, 2.3, and 32.8 h at pH 5.5, 6.0, 6.5, and 7.4, respectively. The degradation half-lives of the cyclohexyl ketal group containing **BHPG-CH-1** at pH 5.5, 6.0, 6.5, and 7.4 were, respectively, 2, 4.7, 13.1, and 138.6 h, respectively. All of these data clearly demonstrate that degradation rates of the polymers can be changed by changing the pH and the structure of ketal groups.

We compared the degradation profiles of BHPGs containing cyclohexyl ketal group and dimethyl ketal groups (Figure 6B,C). A comparison of the degradation of different ketal groups containing HPGs at pH 5.5 is given in Figure 6D. The data show that the degradation of the cyclohexyl ketal group containing HPG was slower than that of the BHPG containing dimethyl ketal groups. For example, the degradation half-lives of **BHPG-DM-1** and **BHPG-CH-1** at pH 5.5 were 0.3 and 2 h, respectively (Table 1). This can be attributed to the difference in the torsional strain involved during the hydrolysis of the cyclohexyl ketal groups in comparison with dimethyl ketal groups.[52,53] As shown in Figure 6D, among the HPGs with different numbers of cyclohexyl ketal groups, **BHPG-CH-3** and **BHPG-CH-4** with three and four cyclohexyl ketal and triazole groups, respectively, degraded at slightly lower rates at pH 5.5 compared with **BHPG-CH-1** with one cyclohexyl ketal group without triazole group and **BHPG-CH-2** with two cyclohexyl ketal and two triazole groups. A similar trend was observed for other pH values greater than 5.5. Below pH 5.5, the rate of degradation was much faster for all polymers. The differences in the degradation rates between the BHPGs containing three and more triazole rings in the initiator core may be due to the increased hydrophobicity of the core structure by the triazole groups, which could possibly change the penetration of water to the core. It has been reported that the degradation of ketal groups could be controlled by varying the hydrophobicity of long chain alkyl groups attached to the ketal moiety.[54] There were no significant differences in the hydrolysis rates between **BHPG-CH-3** and **BHPG-CH-4** containing three and four triazole rings, respectively.

To study the degradation behavior of the BHPGs under in vivo conditions and within cells, the degradation was also studied at 37 °C for the polymers **BHPG-CH-1** and **BHPG-CH-3** at pH 5.5 and 7.4. At both of these pH values the degradation was found to be two to three times faster at 37 °C compared with that at 25 °C (Supporting Information; Figures S18 and S19).

The degradation of BHPG was also studied by gel permeation chromatography. The molecular weights of the BHPGs before and after degradation are given Table 1. The decrease in the molecular weights of degraded BHPG was correlating very well with the number of ketal groups present in the initiator molecules. Therefore, for **BHPG-DM-1**, which contains one ketal group in the polymer chain, the molecular weight decreased from 5200 to 2800 g/mol upon degradation. Similar observations were made for **BHPG-DM-2** and **BHPG-CH-1**, which contain one ketal group, and their molecular weights after degradation were approximately half the original molecular weight. The **BHPG-CH-3** and **BHPG-CH-4** also degraded similarly to low-molecular-weight HPGs, and the decrease in molecular weight was proportional to the number of ketal groups within the polymer (Figure 4). These results together with the low polydispersity and NMR analysis of the BHPGs suggest that the growth of the polymer chains occurred uniformly from the hydroxyl groups of the ketal initiators.

3.4. Biocompatibility Evaluation of BHPGs. *3.4.1. Blood Compatibility of BHPGs.* Hemocompatibility is an important criterion for polymers to be used for vascular applications.[55] Therefore, the newly synthesized BHPGs and their degradation products were evaluated for their blood compatibility by measuring the blood coagulation, complement activation, and platelet activation in presence of polymers. All of the experiments were performed by adding the polymer solutions or degraded polymer solutions in buffer to human plasma/serum.

Blood coagulation in the presence of the BHPGs and their degradation products was measured to investigate their pro- or anticoagulant nature.[56,57] Blood clotting time was measured using clinical clotting assays in the presence of BHPGs. The polymer solutions were incubated with human PPP at 37 °C, and the clotting time was monitored by APTT that measures the time (in seconds) taken for a fibrin clot to form after the addition of partial thromboplastin reagent (actin) and calcium chloride. The APTT of the plasma in the presence of BHPGs and their degradation products was comparable to that of the buffer control (Figure 7A), which shows that these polymers do not cause any adverse effect on blood coagulation. The BHPGs and their degradation products showed a similar profile as that

dx.doi.org/10.1021/bm300959h | *Biomacromolecules* XXXX, XXX, XXX−XXX

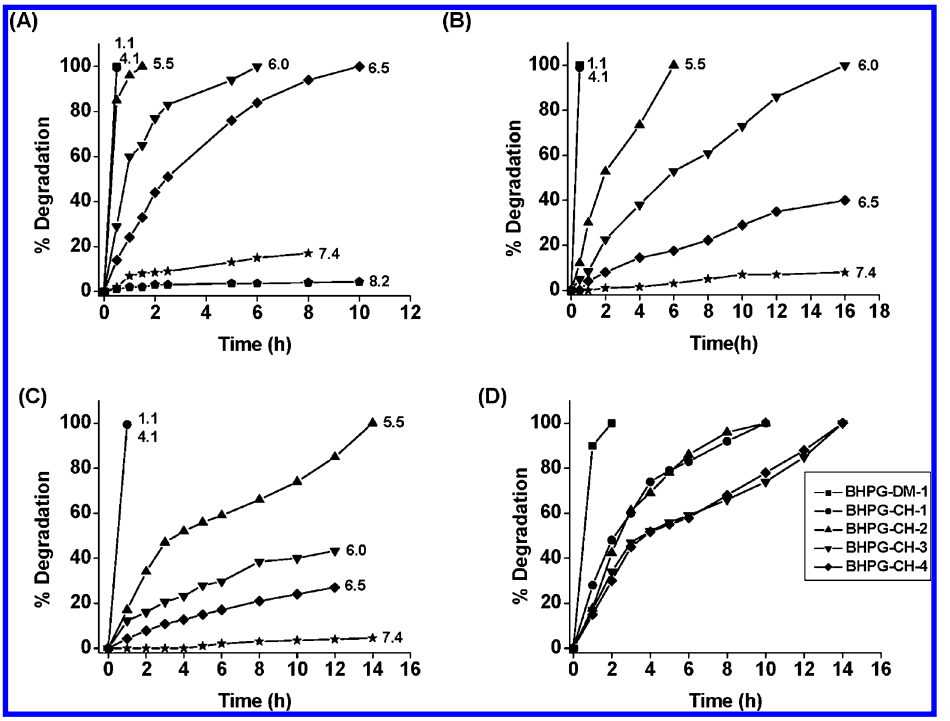

Figure 6. Degradation of core functionalized BHPGs. (A) pH-dependent degradation profiles of **BHPG-DM-1**, (B) **BHPG-CH-1**, and (C) **BHPG-CH-3.** pH values are shown in the Figure. (D) Comparison of the degradation of BHPGs at pH 5.5. The BHPGs degraded rapidly at the acidic pH values (1.1 and 4.1), whereas the degradation was more controlled in the pH 5.5−8.2. BHPGs with cyclohexyl ketal group degraded at much slower rates than those with dimethyl ketal group.

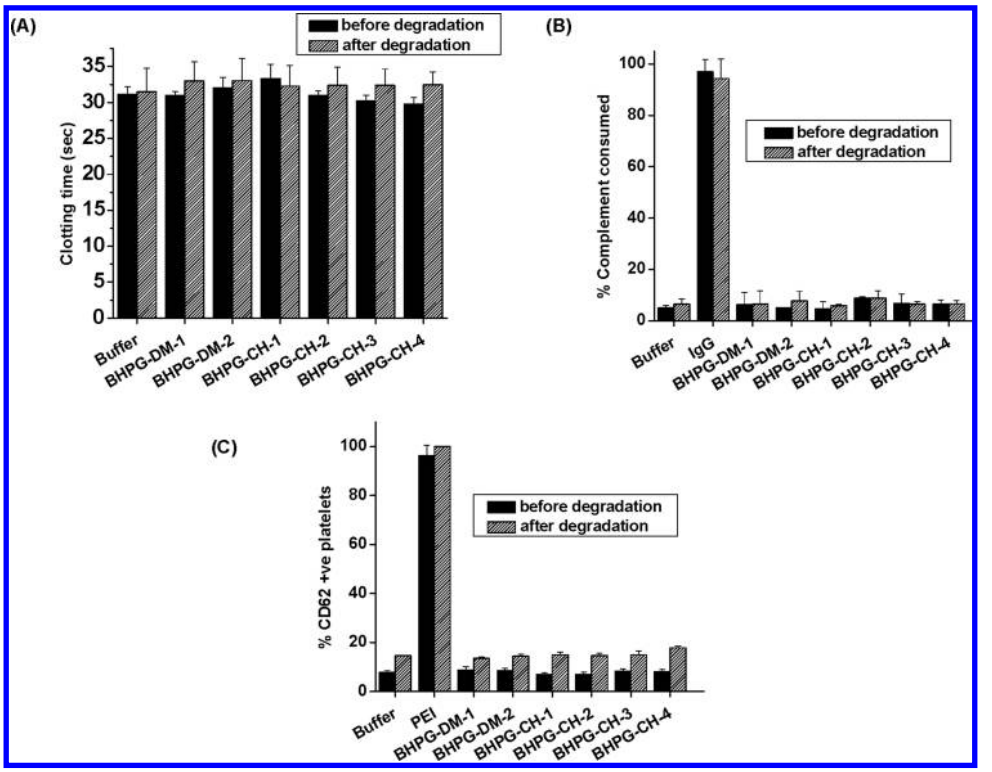

Figure 7. Blood compatibility analysis of BHPGs. (A) Activated partial thromboplastin time (APTT) in human plasma measured at 37 °C. HEPES buffer was used as normal control. (B) Complement activation in human serum measured by CH50 assay using antibody-sensitized sheep RBCs. IgG and HEPES buffer were used as positive and normal controls, respectively. (C) Platelet activation in human-platelet-rich plasma by measuring the expression of activation marker CD62P as measured by flow cytometry. Bovine thrombin and HEPES buffer were used as positive and normal controls, respectively. Final concentration of polymer was 1 mg/mL in all cases.

dx.doi.org/10.1021/bm300959h | *Biomacromolecules* XXXX, XXX, XXX−XXX

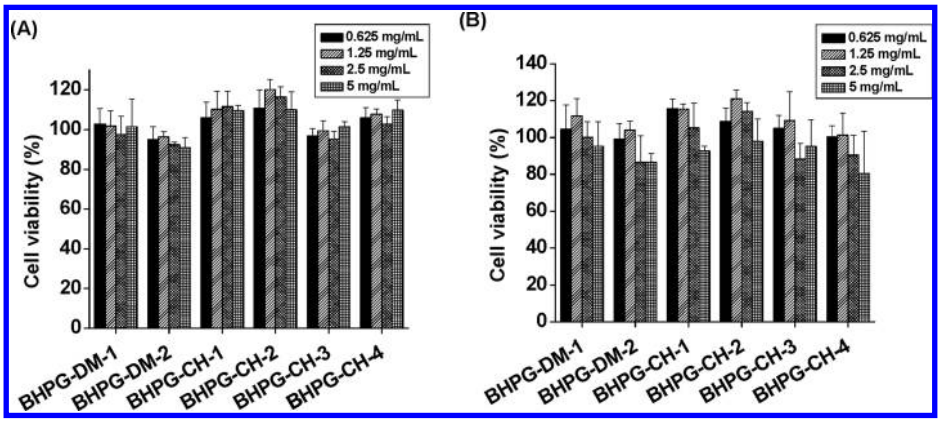

Figure 8. Cell viability of BHPGs (A) and their degradation products (B) against human umbilical vein endothelial cells measured by MTS assay after 48 h of polymer incubation.

of HPGs reported.[58] The slight variation in the buffer controls used for the BHPG and their degradation products was due to the donor variation as these experiments were performed independently at different time points and blood was collected from the different donors. Such donor variation is normal. In each case, a comparison was made between the respective buffer control with the polymers or the degradation products.

Complement activation upon interaction with polymers is an indication of inflammatory potential of the polymer and an indication of blood incompatibility. Activation of the complement system components can lead to several cellular responses such as histamine release and induction of inflammation.[55] The level of complement activation by BHPGs was measured using antibody-sensitized sheep erythrocyte complement consumption assay.[59] The BHPG samples were incubated with human serum at 37 °C for 1 h, and the antibody-sensitized sheep erythrocytes were added to this solution. Lysis of the sensitized sheep erythrocytes was taken as a measure of complement consumption. Erythrocyte lysis was quantified by the amount of hemoglobin released. The level of complement activation by the polymers was compared with that of buffer control and a positive control, immunoglobulin G (IgG) (Figure 7B). Results showed that BHPGs and their degradation products did not activate the complement system, as evident from their insignificant difference in values compared to that of the buffer control.

Platelet activation upon interaction with polymers can result in adverse effects such as thrombotic complications and arterial embolization upon administration of the polymers.[55] Platelet activation by BHPGs was quantified by flow cytometry analysis. The polymer solutions (1 mg/mL, final concentration) were incubated with PRP for 1 h, and platelet activation was measured as expression of platelet activation marker CD62P using monoclonal anti-CD62P-FITC antibody. Platelet activation was expressed as the percentage of platelets that are positive for CD62P. The platelet activation by BHPGs was compared with that of control buffer, and polyethyleneimine (PEI) was used as the positive control. As is evident from Figure 7C, the extent of platelet activation by BHPGs was very similar to that of the buffer control, which indicates that BHPGs and their degradation products did not induce any platelet activation.

3.4.2. Cell Compatibility of BHPGs. Cell compatibility of BHPGs and their degradation products was evaluated by incubating HUVECs with different concentrations of the polymer for 48 h and measuring the number of viable cells by MTS assay. The results are shown in Figure 8, which demonstrates that the BHPGs as well as their degradation products were nontoxic to the cells up to a polymer concentration of 5 mg/mL. This shows the excellent cell compatibility of BHPGs and their degradation products.

4. CONCLUSIONS

We have demonstrated the synthesis of a new class of biodegradable polymers based on core-degradable HPGs by anionic ring-opening polymerization of glycidol using initiators containing acid cleavable ketal linkages. Five different multifunctional initiators containing a varying number hydroxyl groups and ketal groups were synthesized. Both cyclohexyl-ketal- and dimethyl-ketal-group-containing initiators were synthesized. The polymerizations were well-controlled, as evident from the low polydispersities and the monomodal molecular weight distributions of the polymers. The polymers were relatively stable at physiological pH values but exhibited excellent control of degradation at acidic pH values. The degradation rates of these polymers were controlled by varying the structure of ketal groups and number of ketal groups in the initiator. Polymers with cyclohexyl ketal groups in their core showed slower degradation rates than those with dimethyl ketal groups. The BHPGs were degraded to low molecular weights depending on the number of ketal groups present in the BHPG, which indicates that polymerization was occurring uniformly from the hydroxyl groups of the initiators. Blood and cell compatibilities of the BHPGs and their degradation products were excellent. The ability to tune the degradation of BHPGs by varying the ketal group structure in the initiator together with their excellent biocompatibility makes these polymers useful for a variety of drug delivery and bioconjugation applications.

■ ASSOCIATED CONTENT

Supporting Information

NMR spectra of the initiators and polymers, GPC-MALLS traces of the polymers, NMR spectra showing the time-dependent degradation of the BHPGs, and the degradation profiles of the polymers at 37 °C are given. This material is available free of charge via the Internet at http://pubs.acs.org.

dx.doi.org/10.1021/bm300959h | *Biomacromolecules* XXXX, XXX, XXX−XXX

AUTHOR INFORMATION

Corresponding Author

*E-mail: jay@pathology.ubc.ca.

Notes

The authors declare no competing financial interest.

ACKNOWLEDGMENTS

This research was funded by Canadian Institutes of Health Research (CIHR). The LMB Macromolecular Hub at the UBC Centre for Blood Research was funded by Canada Foundation for Innovation and Michael Smith Foundation of Health Research. J.N.K. is a recipient of a CIHR/CBS new investigator in Transfusion Science and Michael Smith Foundation of Health Research Career Investigator Scholar Award.

REFERENCES

(1) Gao, C.; Yan, D. *Prog. Polym. Sci.* **2004**, *29*, 183−275.
(2) Paleos, C. M.; Tziveleka, L. -A.; Sideratou, Z.; Tsiourvas, D. *Expert Opin. Drug Delivery* **2009**, *6*, 27−38.
(3) Zhou, Y.; Huang, W.; Liu, J.; Zhu, X.; Yan, D. *Adv. Mater.* **2010**, *22*, 4567−4590.
(4) Chen, S.; Zhang, X. -Z.; Cheng, S. -X.; Zhou, R. -X.; Gu, Z.-W. *Biomacromolecules* **2008**, *9*, 2578−2585.
(5) Irfan, M.; Seiler, M. *Ind. Eng. Chem. Res.* **2010**, *49*, 1169−1196.
(6) Konkolewicz, D.; Monteiro, M. J.; Perrier, S. *Macromolecules* **2011**, *44*, 7067−7087.
(7) Frey, H.; Haag, R. *Rev. Mol. Biotechnol.* **2002**, *90*, 257−267.
(8) Calderon, M.; Quadir, M. A.; Sharma, S. K.; Haag, R. *Adv. Mater.* **2010**, *22*, 190−218.
(9) Wilms, D.; Striba., S.-E.; Frey, H. *Acc. Chem. Res.* **2010**, *43*, 129−141.
(10) Sunder, A.; Hanselmann, R.; Frey, H.; Mulhaupt, R. *Macromolecules* **1999**, *32*, 4240−4246.
(11) Kainthan, R. K.; Muliawan, E. B.; Hatzikiriakos, S. G.; Brooks, D. E. *Macromolecules* **2006**, *39*, 7708−7717.
(12) Wilms, D.; Wurm, F.; Nieberle, J.; Bohm, P.; Kemmer-Jonas, U.; Frey, H. *Macromolecules* **2009**, *42*, 3230−3236.
(13) Steinhilber, D.; Seiffer, S.; Heyman, J. A.; Paulus, F.; Weitz, D. A.; Haag, R. *Biomaterials* **2011**, *32*, 1311−1316.
(14) Khandare, J.; Mohr, A.; Calderon, M.; Welker, P.; Licha, K.; Haag, R. *Biomaterials* **2010**, *31*, 4268−4277.
(15) Quadir, M. A.; Rodowski, M. R.; Kratz, F.; Licha, K.; Hauff, P.; Haag, R. *J. Controlled Release* **2008**, *132*, 289−294.
(16) Calderon, M.; Graeser, R.; Kratz, F.; Haag, R. *Biorg. Med. Chem. Lett.* **2009**, *19*, 3725−3728.
(17) Calderon., M.; Welker, P.; Licha, K.; Fichtner, I.; Graeser, R.; Haag, R.; Kratz, F. *J. Controlled Release* **2011**, *151*, 295−301.
(18) Kolhe, P.; Khandare, J.; Pillai, O.; Kannan, S.; Leih-Lai, M.; Kannan, R. *Pharm. Res.* **2004**, *21*, 2185−2195.
(19) Zhang, J. G.; Krajden, O. B.; Kainthan, R. K.; Kizhakkedathu, J. N.; Constantinescu, I.; Brooks, D. E.; Gyongyossy-Issa, M. I. C. *Bioconjugate Chem.* **2008**, *19*, 1241−1247.
(20) Papp, I.; Dernedde, J.; Enders, S.; Haag, R. *Chem. Commun.* **2008**, *44*, 5851−5853.
(21) Kizhakkedathu, J. N.; Creagh, L. A.; Shenoi, R. A.; Rossi, N. A. A.; Brooks, D. E.; Chan, T.; Lam, J.; Dandepally, S. R.; Haynes, C. A. *Biomacromolecules* **2010**, *11*, 2567−2575.
(22) Papp, I.; Dernedde, J.; Enders, S.; Riese, S. B.; Shiao, T. C.; Roy, R.; Haag, R. *ChemBioChem* **2011**, *12*, 1075−1083.
(23) Kainthan, R. K.; Janzen, J.; Kizhakkedathu, J. N.; Devine, D. V.; Brooks, D. E. *Biomaterials* **2008**, *29*, 1693−1704.
(24) Kainthan, R.; Mugabe, C.; Burt, H. M.; Brooks, D. E. *Biomacromolecules* **2008**, *9*, 886−895.
(25) Mugabe, C.; Hadaschik, B. A.; Kainthan, R. K.; Brooks, D. E.; So, A. I.; Gleave, M. E.; Burt, H. M. *BJU Int.* **2009**, *103*, 978−986.
(26) Burakowska, E.; Haag, R. *Macromolecules* **2009**, *42*, 5545−5550.
(27) Burakowska, E.; Zimmerman, S. C.; Haag, R. *Small* **2009**, *5*, 2199−2204.
(28) Burakowska, E.; Quinn, J. R.; Zimmerman, S. C.; Haag, R. *J. Am. Chem. Soc.* **2009**, *131*, 10574−10580.
(29) Kainthan, R. K.; Gnanamani, M.; Ganguli, M.; Ghosh, T.; Brooks, D. E.; Maiti, S.; Kizhakkedathu, J. N. *Biomaterials* **2006**, *27*, 5377−5390.
(30) Fischer, W.; Quadir, M. A.; Barnard, A.; Smith, S. K.; Haag, R. *Macromol. Biosci.* **2011**, *11*, 1736−1746.
(31) Turk, H.; Haag, R.; Alban, S. *Bioconjugate Chem.* **2004**, *15*, 162−167.
(32) Dernedde, J.; Rausch, A.; Weinhart, M.; Enders, S.; Tauber, R.; Lich, K.; Schirner, M.; Zugel, U.; von Bonin, A.; Haag, R. *Proc. Natl. Acad. Sci. U.S.A.* **2010**, *107*, 19679−19684.
(33) Weinhart, M.; Groger, D.; Enders, S.; Dernedde, J.; Haag, R. *Biomacromolecules* **2011**, *12*, 2502−2011.
(34) Rossi, N. A. A.; Constantinescu, I.; Brooks, D. E.; Scott, M. D.; Kizhakkedathu, J. N. *J. Am. Chem. Soc.* **2010**, *132*, 3423−3430.
(35) Rossi, N. A. A.; Constantinescu, I.; Kainthan, R. K.; Brooks, D. E.; Scott, M. D.; Kizhakkedathu, J. N. *Biomaterials* **2010**, *31*, 4167−4178.
(36) Chapanian, R.; Constantinescu, I.; Brooks, D. E.; Scott, M. D.; Kizhakkedathu, J. N. *Biomaterials* **2012**, *33*, 3047−3057.
(37) Kleifield, O.; Doucet, A.; auf dem Keller, U.; Prudova, A.; Schilling, O.; Kainthan, R. K.; Starr, A. E.; Foster, L. J.; Kizhakkedathu, J. N.; Overall, C. M. *Nat. Biotechnol.* **2010**, *28*, 281−288.
(38) Baudette, P.; Rossi, N. A. A.; Huesgen, P. F.; Yu, X.; Shenoi, R. A.; Doucet, A.; Overall, C. M.; Kizhakkedathu, J. N. *Anal. Chem.* **2011**, *83*, 6500−6510.
(39) Yu, X.; Liu, Z.; Janzen, J.; Chafeeva, I.; Horte, S.; Chen, W.; Kainthan, R. K.; Kizhakkedathu, J. N.; Brooks, D. E. *Nat. Mater.* **2012**, *11*, 468−476.
(40) Kainthan, R. K.; Brooks, D. E. *Biomaterials* **2007**, *28*, 4779−4787.
(41) Steinhilber, D.; Sisson, A. L.; Mangoldt, D.; Welker, P.; Licha, K.; Haag, R. *Adv. Funct. Mater.* **2010**, *20*, 4133−4138.
(42) Duncan, R. *Anti-Cancer Drugs* **1992**, *3*, 175−210.
(43) Stubbs, M.; McSheehy, P. M. J.; Griffiths, J. R.; Bashford, C. L. *Mol. Med. Today.* **2000**, 15−19.
(44) Edinger, D.; Wagner, E. *Nanomed. Nanobiotechnol.* **2011**, *3*, 33−46.
(45) Roux, E.; Francis, M.; Winnik, F. M.; Leroux, J. *Int. J. Pharm.* **2002**, *242*, 25−36.
(46) Ulbrich, K.; Subr, V. *Adv. Drug Delivery Rev.* **2004**, *56*, 1023−1050.
(47) Shenoi, R. A.; Jayaprakash, K. N.; Hamilton, J. H.; Lai, B. F. L.; Horte, S.; Kainthan, R. K.; Varghese, J. P.; Rajeev, K. G.; Manoharan, M.; Kizhakkedathu, J. N. *J. Am. Chem. Soc.* **2012**, DOI: 10.1021/ja305080f.
(48) Oikawa, M.; Wada, A.; Okazaki, F.; Kusumoto, S. *J. Org. Chem.* **1996**, *61*, 4469−4471.
(49) Hooper, N.; Beeching, L. J.; Dyke, J. M.; Morris, A.; Ogden, J. S.; Dias, A. A.; Costa, M. L.; Barros, M. T.; Cabral, M. H.; Moutinho, A. M. C. *J. Phys. Chem. A* **2002**, *106*, 9968−9975.
(50) Wohl, R. A. *Synthesis* **1974**, *1*, 38−40.
(51) Andre, S.; Lahmann, M.; Gabius, H.-J.; Oscarson, S. *Mol. Pharmaceutics* **2010**, *7*, 2270−2279.
(52) Kreevoy, M. M.; Morgan, C. R.; Taft, R. W., Jr. *J. Am. Chem. Soc.* **1960**, *82*, 3064−3066.
(53) Deslongchamps, P.; Dory, Y. L.; Li, S. *Tetrahedron* **2000**, *56*, 3533−3537.
(54) Yang, S. C.; Bhide, M.; Crispe, I. N.; Pierce, R. H.; Murthy, N. *Bioconjugate Chem.* **2008**, *19*, 1164−1169.
(55) Gobert, M. B.; Sefton, M. V. *Biomaterials* **2004**, *25*, 5681−5703.
(56) Hansson, K. M.; Tosatti, S.; Isaksson, J.; Wettero, J.; Texter, M.; Lindahl, T. L. *Biomaterials* **2005**, *26*, 861−872.
(57) Amarnath, L. P.; Srinivas, A.; Ramamurthi, A. *Biomaterials* **2006**, *27*, 1416−1424.

(58) Kainthan, R. K.; Hester, S. R.; Levin, E.; Devine, D. V.; Brooks, D. E. *Biomaterials* **2007**, *28*, 4581−4590.
(59) Inglis, J. E.; Radziwon, K. A.; Maniero, G. D. *J. Physiol. Educ.* **2008**, *32*, 317−321.